SUPPORTING INFORMATION

Novel insights into the taxonomic diversity and molecular mechanisms of bacterial Mn(III) reduction

Nadia Szeinbaum[1,2,6‡], Brook L. Nunn[3], Amanda R. Cavazos[2], Sean A. Crowe[2,4], Frank J. Stewart[1,5], Thomas J. DiChristina[1], Christopher T. Reinhard[2,6], and Jennifer B. Glass[2,6*]

[1]School of Biological Sciences, Georgia Institute of Technology, Atlanta, GA, USA

[2]School of Earth and Atmospheric Sciences, Georgia Institute of Technology, Atlanta, GA, USA

[3]Department of Genome Sciences, University of Washington, Seattle, WA, USA

[4]Department of Microbiology & Immunology and Department of Earth, Ocean, & Atmospheric Sciences, University of British Columbia, Vancouver, Canada

[5]Department of Microbiology and Immunology, Montana State University, Bozeman, Montana

[6]NASA Astrobiology Institute, Alternative Earths Team, Mountain View, CA

[‡]Now at Beyond Meat, El Segundo, CA

*Corresponding author: jennifer.glass@eas.gatech.edu

Running title: Novel undecaheme in Betaproteobacteria

Content:

1. Experimental procedures

Source of inoculum. Lake Matano is a metal-rich, ancient ocean analog with an active Mn cycle (1, 2). Organic carbon in Lake Matano is mostly mineralized via methanogenesis (3). A 15-cm sediment core from 200 m water depth in Lake Matano, Sulawesi Island, Indonesia (02°26′27.1″S, 121°15′12.3″E; *in situ* sediment temperature ~27°C) was sampled in November 2014 and sub-sampled at 2.5-cm increments. Sediments were sealed in gas-tight Mylar bags with no headspace (4) and stored at 4°C for ~1 year.

Inoculation of enrichment cultures. Mylar bags containing sediment samples were opened in an anoxic chamber (97% N_2 and 3% H_2; Coy Laboratory Products, Grass Lake, MI, USA). Sediments from each 2.5 cm subsample were transferred to 160 mL serum bottles, diluted 1:2 with minimal media, and pre-incubated for 45 days at 30°C in 100% N_2 headspace to deplete endogenous organic carbon, electron donors, and electron acceptors. Sediments from the top 5 cm were subsequently mixed together and transferred to defined medium at a 1:20 dilution (transfer 1, day 45) amended with Mn(III) and a headspace of CH_4:N_2 (50:50) or N_2. Subsequent transfers were carried out in the same way (transfer 2, day 91; transfer 3, day 183; transfer 4, day 230) for CH_4 headspace cultures, with heat-killed and substrate controls generated each time using the newly transferred culture (10% v/v dilution). By day 210, enrichments appeared to be sediment-free, except for microparticles. The fifth transfer (day 245) inoculated using non-labeled methane, was used entirely for metaproteomic analysis after visual confirmation of active Mn(III) reduction in the live enrichment bottles (see **Figs. 1**, **S1**). Two 100 mL bottles were pooled together two obtain 200 mL duplicates for each treatment, centrifuged (10,000 x g, 30

46 min, 4°C) and supernatant-free pellets were stored at -80°C until protein extraction and
47 metaproteomic sequencing**.**

48 Defined medium consisted of modified artificial freshwater medium lacking nitrate and
49 sulfate, developed based on the pore water composition of Lake Matano sediments as described
50 in prior work (5). The medium contained 3 mM $NaHCO_3$, 825 µM $MgCl_2$, 550 µM $CaCO_3$, 225
51 µM NH_4Cl, 5 µM Na_2HPO_4, 3.5 µM K_2HPO_4, and a trace metal solution (1 nM $CuCl_2$, 1.5 nM
52 Na_2MoO_4, 2.5 nM $CoCl_2$, 23 nM $MnCl_2$, 9 nM $FeCl_3$, 4 nM $ZnCl_2$, 0.091 µg/L vitamin B_{12},
53 0.091 µg/L biotin, and 18.18 µg/L thiamine. Vitamins were filter-sterilized and added after
54 autoclaving. Bottles were stoppered with sterile black bromobutyl stoppers (Geo-Microbial
55 Technologies, Ochelata, OK, USA; pre-boiled in 0.1 N NaOH), and crimped with aluminum
56 seals. An acetate-free 10 mM stock of Mn(III)-pyrophosphate was prepared using solid Mn_2O_3
57 (99% purity, 325 mesh powder, Sigma Aldrich) instead of Mn(III)-acetate (6) and filter-
58 sterilized. Mn(III)-pyrophosphate was added at a final concentration of 1 mM. Bottles were
59 purged with 99.9% N_2 for 20 min, and were appropriate, CH_4 was injected with a 50% headspace
60 volume of CH_4 at a 1:1 labeled to unlabeled ratio (99.9% CH_4 and 99% $^{13}CH_4$; Cambridge
61 Isotope Laboratories, Tewksbury, MA, USA). Heat-killed controls were autoclaved prior to
62 Mn(III) or CH_4 addition. All treatments were duplicated, and bottles were incubated in the dark
63 at 30°C.

64 **Substrate utilization.** The benzidine method was used to measure Mn(III) consumption
65 (7) throughout the transfer 4 enrichment. Methane ($^{13}CH_4$) oxidation was monitored by
66 measuring ^{13}C enrichment in dissolved inorganic carbon as described in (5).

67 **16S rRNA gene amplicon sequencing.** To identify the dominant microbial community
68 members, we analyzed the microbial community composition of samples taken at the end of each

69 enrichment period by sequencing 16S rRNA gene amplicons as described previously (5). Reads
70 were analyzed using Mothur (8) following its MiSeq standard operating procedure
71 (https://www.mothur.org/wiki/MiSeq_SOP, accessed November 2017). Merged reads were
72 dereplicated and aligned to the ARB SILVA SSU database release 123 (July 23, 2015).
73 Homopolymers longer than 8bp were filtered out. Reads were then clustered into OTUs at 97%
74 similarity based on uncorrected pairwise distance matrices. OTUs were classified using the ARB
75 SILVA SSU reference taxonomy database release 123.
76 **Metagenome (DNA) sequencing and assembly.** Community DNA was processed using
77 the Nextera XT DNA Sample Prep kit and sequenced using a paired-end Illumina MiSeq 600 kit.
78 Raw reads were submitted to NCBI. The accessions for the study and samples in the submission
79 are PRJNA489678, LakeMatanoMn3_Enrichment (SAMN10343573). The accession numbers
80 for the N_2 headspace experiment and run are LM_Mn(III)_2018 (SRX5007804) and
81 LakeMatano_11_NoMethane_R1.fastq.gz (SRR8188020), and the accession numbers for the
82 CH_4 headspace experiment and run are LM_Mn(III)_CH4_2018 (SRX5007805) and
83 LakeMatano_9_Methane_R1.fastq.gz (SRR8188019).
84 Barcoded sequences were de-multiplexed, trimmed (length cutoff 100 bp), and filtered to
85 remove low quality reads (average Phred score <25) using Trim Galore!
86 (http://www.bioinformatics.babraham.ac.uk/projects/trim_galore/). Forward and reverse reads
87 were assembled using SPAdes (9) with the 'meta' option. Metagenomic reads were deposited in
88 NBCI. Contigs ≥ 500 nt were organized into MAGs based on tetranucleotide frequency and
89 sequence coverage using MaxBin 2.0 (10). MAG completeness and contamination were
90 estimated by lineage-specific marker genes using CheckM (11). We obtained one
91 *Betaproteobacteria* metagenome-assembled genome (MAG; *Rhodocyclales* bacterium GT-UBC,

NCBI accession QXPY01000000) with 99.53% completeness, 0.02% contamination, 60.9% GC content, and 4,555 protein-coding genes. We provisionally classified *Rhodocyclales* bacterium GT-UBC as a new species within the *Dechloromonas* genus, which we named "*Candidatus* Dechloromonas occultata" sp. nov.; etymology: occultata; (L. fem. adj. 'hidden'), based on its resistance to cultivation. We also obtained one *Deltaproteobacteria* MAG (*Desulfuromonadales* bacterium GT-UBC; NCBI accession RHLS01000000) with 99.36% completeness, 0.64% contamination, 59.9% GC content, 3,617 protein-coding genes, and 80% ANI to *Geobacter sulfurreducens.* We provisionally named *Desulfuromonadales* bacterium GT-UBC "*Candidatus* Geobacter occultata" sp. nov.

Comparative genomic analysis. The "*Ca*. D. occultata" MAG was annotated using RAST. Metabolic pathways were identified in RAST (12-14), and manually checked for completeness in PATRIC (15), following pathways reported in KEGG (https://www.genome.jp/kegg/) and MetaCyc (https://metacyc.org/) and confirming potential new variants in the literature (references where appropriate throughout the manuscript). For incomplete pathways, the three other genomes of isolated *Dechloromonas* strains (*D. aromatica*, *D. denitrificans*, and *D. agitata*) in PATRIC were searched for missing proteins. Central metabolic and secondary pathways were compared among *Dechloromonas* spp. and other metal-cycling species using the RAST subsystems option, searching for specific annotated proteins with RAST, and within PATRIC using the Compare Region Viewer and its heatmap options. Proteins of interest were characterized *in silico* based on conserved domains and homology searches with BLAST and NCBI tools. Localization of proteins was predicted using PSORTb model ECSVM (16). The synteny of gene clusters containing functional genes of interest were analyzed using Simple Synteny (https://www.dveltri.com/simplesynteny/cfinder.html, last

accessed July 2018). Putative multiheme *c*-type cytochromes (≥3 Cxx(x)CH motifs) were identified using a previously reported Python script (https://github.com/bondlab/scripts, (17)).

Phylogenetic analysis. The evolutionary history of functional genes was inferred using MEGA7 (18) with the Maximum Likelihood method based on the JTT matrix-based model (19). After all gaps were eliminated, initial tree(s) for the heuristic search were obtained automatically by applying Neighbor-Join and BioNJ algorithms to a matrix of pairwise distances estimated using a JTT model, and then selecting the topology with superior log likelihood value. The trees were drawn to scale, with branch lengths measured in the number of substitutions per site and bootstrap values based on 500 replicates. The synteny of selected genes was determined using Simple Synteny (20). The evolutionary history of selected whole genomes of Proteobacteria was reconstructed using GToTree (21) with genomic NCBI IDs as input, retrieved manually. Single-copy genes (SCGs) were identified from a set of 74 single-copy genes. GToTree uses concatenated alignments of identified SCGs to build the phylogenomic tree with FastTree. The final tree was viewed and edited in FigTree V1.4.4 (22).

Protein digestion and desalting. To solubilize oxidized metal precipitants and precipitate proteins, 100 µL of 20% trichloroacetic acid (4°C) was added to each sample and incubated on ice for 1 hour. Bacterial cells and soluble proteins were pelleted at 10,000 x g (1 hr, 4°C). Cells were then resuspended in 100 µL of 6 M urea in 50 mM NH_4HCO_3 and lysed using a sonicating probe (3 watts; 15s, 5 times), alternating in dry ice in ethanol to keep the sample cold. Sonication, digestion, and desalting proceeded as previously described (23). Briefly, after sonication and protein quantification using the Bradford assay (Bio-Rad, Hercules, CA), tris(2-carboxyethyl)phosphine (TCEP) was added to reduce samples (1 hr, 37°C), and iodoacetamide was used as the alkylating agent (1hr, in dark, RT). NH_4HCO_3 and HPLC-grade methanol were

added to each sample to dilute the urea to allow the trypsin digestion to proceed. Trypsin was added in a 1:20 ratio and incubated overnight at RT. The digestion was stopped by adding small aliquots of 10% formic acid until a pH < 2 was achieved. Prior to desalting the peptides, samples were dried down and reconstituted in 5% acetonitrile with 0.1% trifluoroacetic acid. Desalting was carried out with MicroSpin C18 columns following the manufacturer's instructions (The Nest Group). Peptides were dried and reconstituted in 5% ACN with 0.1% formic acid to achieve concentrations of 2 $\mu g\ \mu L^{-1}$.

LC-MS/MS. The mass spectrometry analysis was performed on a QExactive at the University of Washington Proteomics Resource (Seattle, WA). Samples were separated and introduced into the mass spectrometer (MS) by reverse-phase chromatography using a Manufactured PicoTip fused silica capillary column (30 cm long, 75 µm i.d.) packed with C18 particles (Dr. Maisch ReproSil-Pur; C18-Aq, 120 Å, 3 µm) fitted with a 3 cm long, 100 µm i.d. precolumn (Dr. Maisch ReproSil-Pur; C18-Aq, 120 Å, 3 µm). Peptides were eluted using an acidified (formic acid, 0.1% v/v) water-acetonitrile gradient (5–35% acetonitrile in 90 min) and mass spectrometry was performed on a Thermo Fisher (San Jose, CA) QExactive (QE). The top 20 most intense ions were selected for MS2 acquisition from precursor ion scans of 400–1200 $m\ z^{-1}$. Centroid full MS resolution data was collected at 70,000 with AGC target of 1E6 and centroid MS2 data was collected at resolution of 35,000 with AGC target of 5E4. Dynamic exclusion was set to 15 seconds and +2, +3, +4 ions were selected for MS2 using data dependent acquisition mode (DDA). Quality control (QC) peptide mixtures were analyzed every fifth injection to monitor chromatography and MS sensitivity. Skyline was used to determine that QC standards did not deviate >10% through all analyses (24). The mass spectrometry data were deposited to the ProteomeXchange Consortium via the PRIDE partner repository with the dataset

identifier PXD011642.

Protein identification and data analyses. Peptide identifications from mass spectrometry data were completed using Comet (25). The protein database used for correlating spectra with protein identifications was generated from the metagenome by Prokka (26), and from each individual bin using RAST (13) and included the MAGs to improve peptide spectra correlations (15). This was then combined with 50 common contaminants and the QC peptides. Comet parameters included: reverse concatenated sequence database search, trypsin enzyme specificity, cysteine modification of 57 Da (resulting from the iodoacetamide) and modifications on methionine of 15.999 Da (oxidation). Concatenated target–decoy database searches were completed and minimum protein and peptide thresholds were set at $P > 0.95$ on ProteinProphet and $P > 0.99$ on PeptideProphet (27). Protein identifications from the whole-cell lysates were accepted by ProteinProphet if the above mentioned thresholds were passed, two or more peptides were identified (PeptideProphet), and at least one terminus was tryptic (27). Calculated false discovery rates (FDR) were <0.01. Resulting data files were combined and normalized spectral abundances were calculated in QPROT with Abacus (28). Abacus parameters include initial probability threshold of 0.5 on peptides, and a minimum protein probability of 0.8. Abacus provides consistent protein inferences across biological and technical replicates. Abacus spectral abundance outputs were analyzed with QSpec, a statistical framework within QPROT, to determine log fold changes between treatments. Log fold change in protein abundances calculated using QSpec were accepted if ≥ 0.5 and Zstatistic score ≥ 2.0 (increased abundance across all replicates) or ≤ -0.5 and Zstatistic score ≤ -2.0 (decreased abundance across all replicates) (28). Peptide counts were normalized to total peptide counts for each treatment. Averages of normalized technical replicates were used to compare treatments with and without

methane. A two-tailed paired t-test was carried out using Excel to test the null hypothesis of no differential expression among treatments and determine the p-value associated with each change.

Cultivation attempts. Isolation strategies were designed considering the metabolic potential of "*Ca.* D. occultata" but failed to isolate the targeted organism. Samples from highly enriched cultures were inoculated with acetate for denitrification or microaerobic Fe(II) oxidation. For Fe(II) oxidation, samples were inoculated into two-layered FeS vs. O_2 gradient tubes (29), with 1 mM acetate in the top layer. There was no Fe(II) oxidation in Mn(III)-amended treatments. With O_2 addition, visual evidence for Fe(II) oxidation was observed, and a *Comamonas* spp. with closest hits to environmental sequences from lake sediment was isolated. With acetate and Mn(III), a *Comamonas aquatica* strain was isolated.

1. Supplemental Tables

Table S1. Average nucleotide identity of *Dechloromonas* species. Numbers in the table indicate percentage of whole genome nucleotide identity.

	Dechloromonas sp. UBA6271	*Dechloromonas denitrificans* ATCC BAA-841	*Dechloromonas aromatica* RCB	*Dechloromonas* sp. GT-UBC1	*Dechloromonas agitata* is5	*Dechloromonas* sp. UBA5022
Dechloromonas sp. UBA6271	100.00					
Dechloromonas denitrificans ATCC BAA-841	80.46	100.00				
Dechloromonas aromatica RCB	80.58	82.14	100.00			
Dechloromonas sp. strain GT-UBC1	79.65	82.36	80.92	100.00		
Dechloromonas agitata is5	79.28	81.42	81.59	80.80	100.00	
Dechloromonas sp. UBA5022	81.42	82.74	81.90	81.37	81.11	100.00

Table S2. List of multiheme cytochromes encoded by "*Candidatus* Dechloromonas occultata". Those in bold indicate expressed proteins (see **Table 1**).

NCBI ID	Predicted function	Heme-binding motifs	Protein length (aa)
RIX41009	**NapC-like**	**4**	**207**
RIX43626	NapC-like	4	198
RIX48944	**MtoA-2**	**10**	**320**
RIX49874	**MtoA-1**	**10**	**331**
RIX49876	Hypothetical protein	3	127
RIX49688	**OccA**	**3**	**327**
RIX49689	**OccB**	**3**	**343**
RIX49878	OccD	3	175
RIX49691	**OccF**	**4**	**289**
RIX49694	**OccI**	**3**	**139**
RIX49879	**OccJ**	**4**	**338**
RIX49695	OccL	3	194
RIX49881	OccM	3	87
RIX49697	**OccP**	**11**	**922**
RIX49727	Hypothetical protein	5	695

Table S3. Genomes containing MtoA, OccP, NapA, NirS, NorB, or cNosZ homologs in Alpha-, Beta-, and Gammaproteobacteria. "Ecosystem Type" refers to the source of inoculum for pure cultures or the source of environmental DNA for assembled genome of uncultured organisms. Spreadsheet is attached as supplemental file.

Table S4. Expression levels for "*Ca*. D. occultata" proteins during Mn(III) reduction with and without CH_4. Peptide counts are normalized to total "*Ca*. D. occultata" proteins x 10,000. Blank cells indicate proteins with <5 normalized peptide counts. Gray boxes indicate membrane proteins with that may be underrepresented by proteomic analyses. SP: signal peptide (Y:present/N:absent); TMH: numbers of transmembrane helices; # CxxCH: number of heme-binding motifs; P-sort: predicted cellular location. P: periplasm, C: cytoplasm; OM: outer membrane; IM: inner membrane, E: extracellular; U: unknown. Spreadsheet is attached as supplemental figure.

2. Supplemental Figures

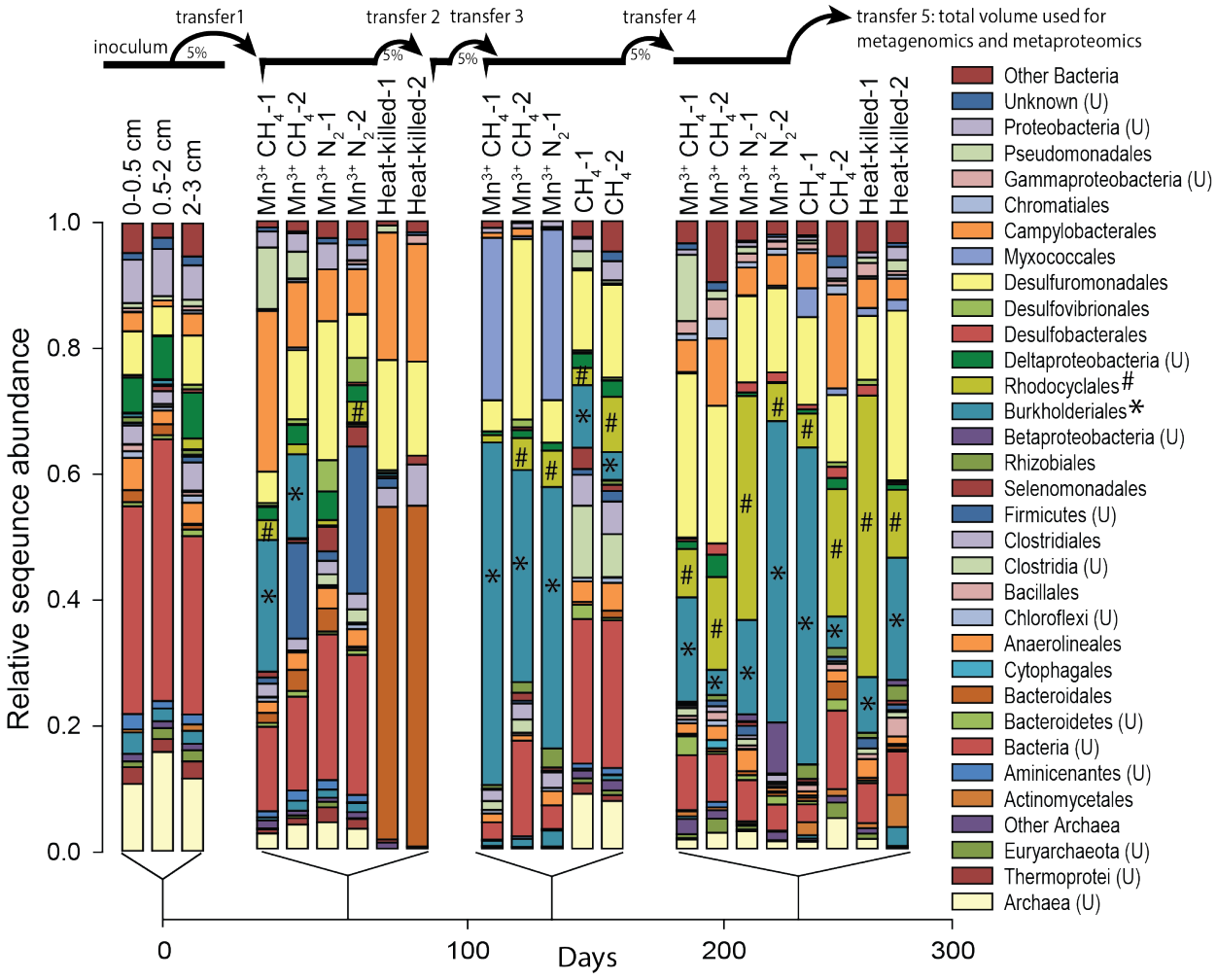

Figure S1. Taxonomic succession in enrichment culture. Relative abundance of taxa enriched from samples from Lake Matano sediments over a 335-day period, based on ~200 bp 16S rRNA gene amplicon sequences. Only live treatments with CH_4 and Mn(III) were transferred. (U) indicates unclassified taxa.

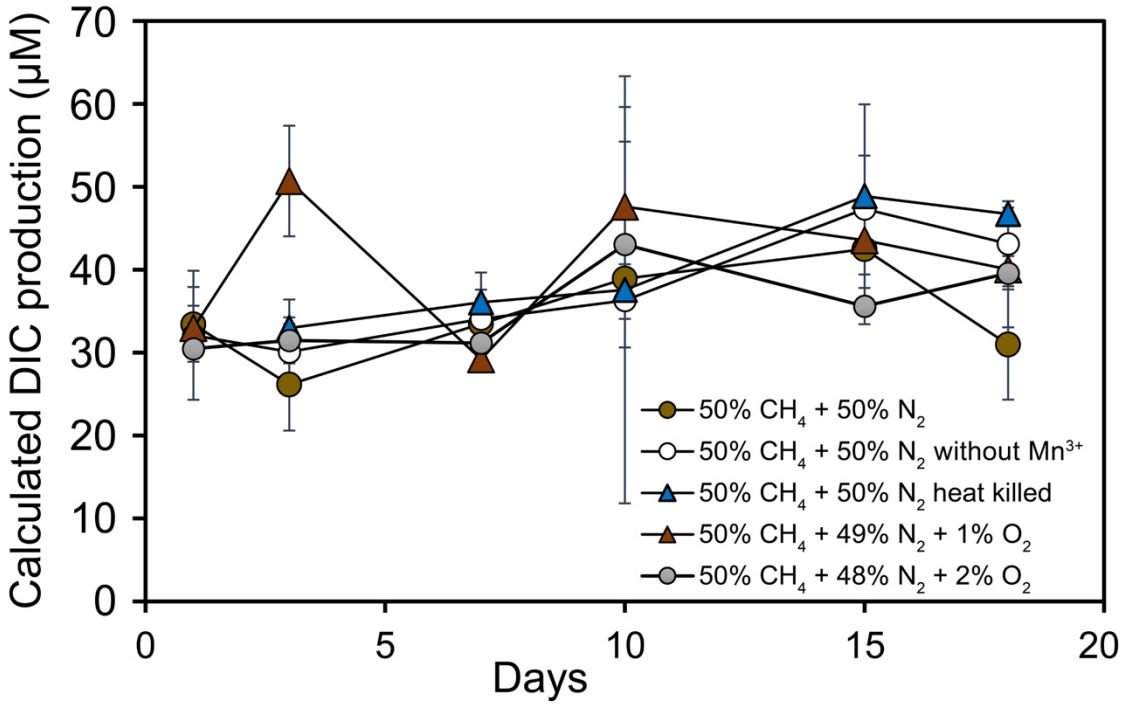

227

228 **Figure S2. Methane oxidation after the fourth transfer of enrichment cultures.** This graph

229 shows the concentration of methane-derived dissolved inorganic carbon (DIC) in sediment

230 enrichments amended with $^{13}CH_4$, calculated based on isotopic enrichment values and total DIC

231 based on (30). Errors bars represent standard deviation of duplicate measurements.

232

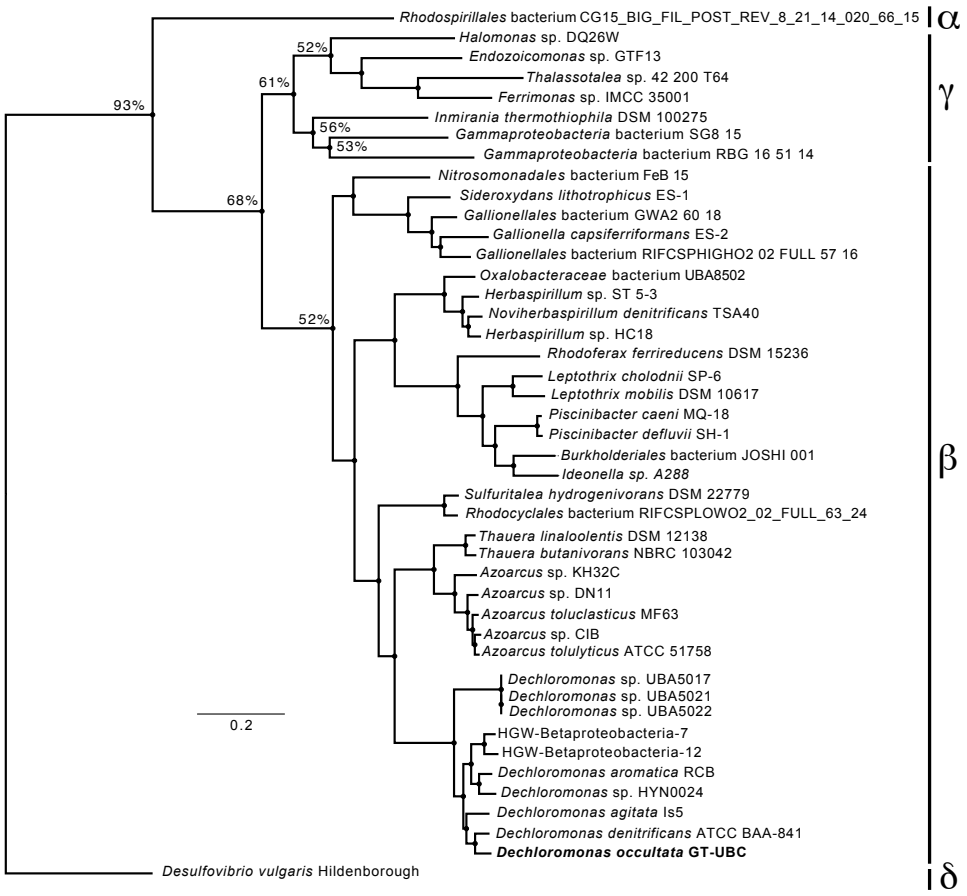

Figure S3. Phylogeny of "*Candidatus* Dechloromonas occultata" MAG. The phylogenic placement of the "*Ca*. D. occultata" MAG was compared to genomes of *Alphaproteobacteria*, *Betaproteobacteria* and *Gammaproteobacteria*, with *occP* and/or *mtoA* homologs **(Table S3)**. Environmental MAGs for uncultivated species are labeled with IDs. Genomes without *occP* on the phylogeny included *Dechloromonas denitrificans* (GCA_001551835.1), *Dechloromonas agitata* is5 (GCA_000519045.1), *Dechloromonas* UBA 5017 (GCA_002396525.1), *Dechloromonas* UBA 5021 (GCA_002396725.1), and *Dechloromonas* UBA 5022 (GCA_002396465.1). The deltaproteobacterium *Desulfovibrio vulgaris* was used as the outgroup (GCA_000195755.1). Bootstrap values over 50 are shown. GenBank assembly accession numbers are given in **Table S3**.

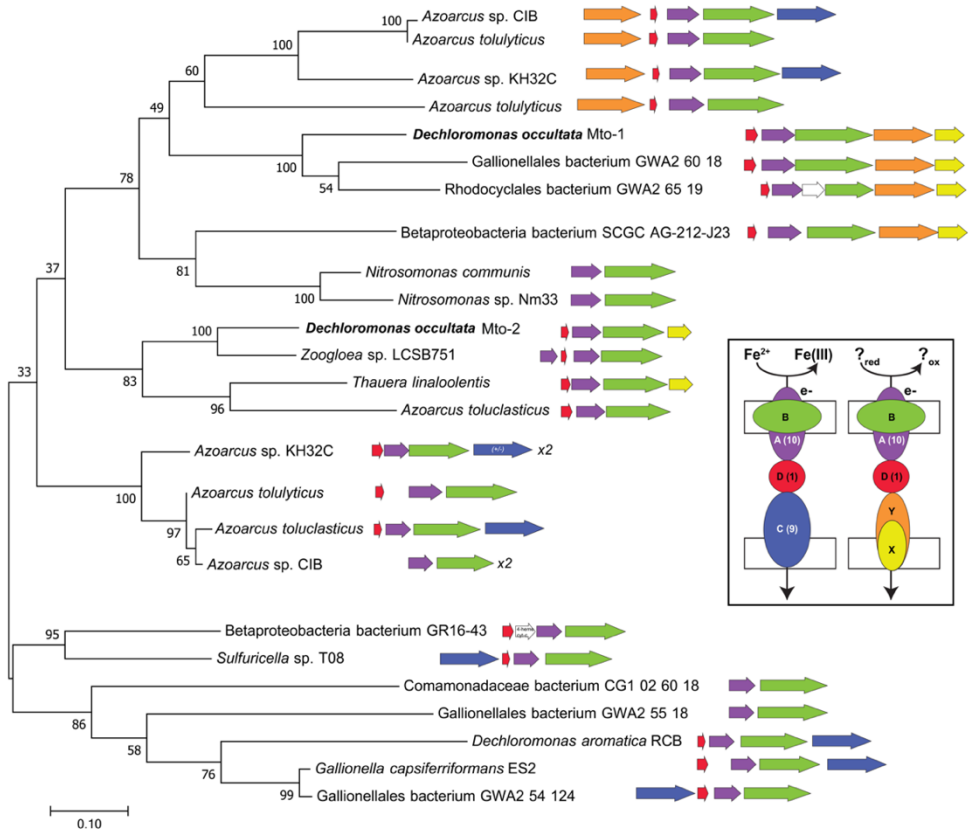

Figure S4. Phylogeny of decaheme c-type cytochrome MtoA and synteny of Mto loci. Maximum likelihood phylogeny of the MtoA protein sequence from "*Ca*. D. occultata" in relationship to other MtoA homologs from *Beta-* and *Gammaproteobacteria*. Accession numbers are given in **Table S3**. Bootstrap support is based on 500 samples. Next to each branch is the genomic organization of *mtoA* and neighboring genes in each species, color-coded to represent function and predicted cellular locations. Species with duplicated clusters are annotated as "x2". Inset: left, canonical Mto pathway; right: proposed alternative Mto pathway in "*Ca*. D. occultata" and other uncultured *Betaproteobacteria*; the labels A, B, C, D, X, and Y correspond to MtoA, MtoB, MtoC, MtoX and MtoY, respectively, with heme counts in parentheses. OM: outer membrane; IM: inner membrane.

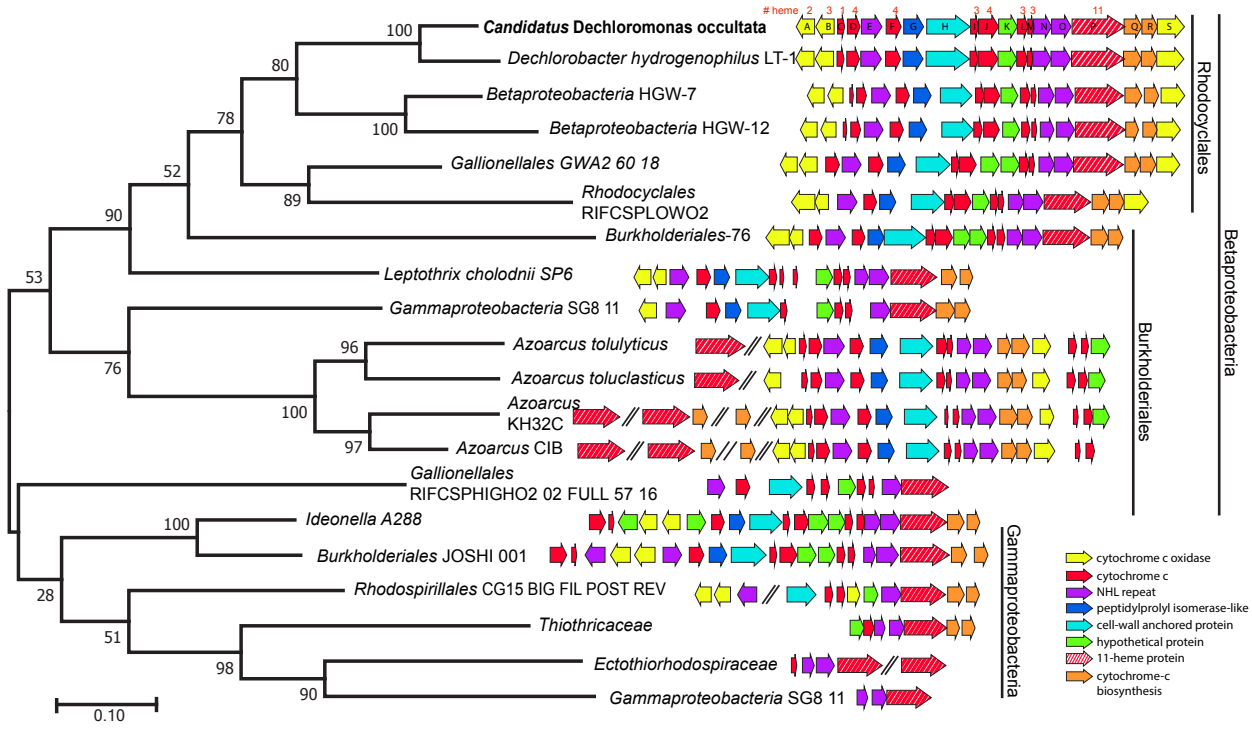

Figure S5. Phylogeny of undecaheme c-type cytochrome OccP and synteny of Occ loci. The tree represents the evolutionary history of the OccP protein from "*Ca*. D. occultata" in relationship to other OccP homologs from Beta- and *Gammaproteobacteria*. Accession numbers are given in **Table S3**. Note that *Gammaproteobacteria* bacterium SG8-11 contains multiple copies of the *occ* operon, one of which is within the *Burkholderiales* clade. Branch lengths represent substitutions per site. Next to each branch is the genomic organization of OccP and neighboring genes in each strain, color-coded by function.

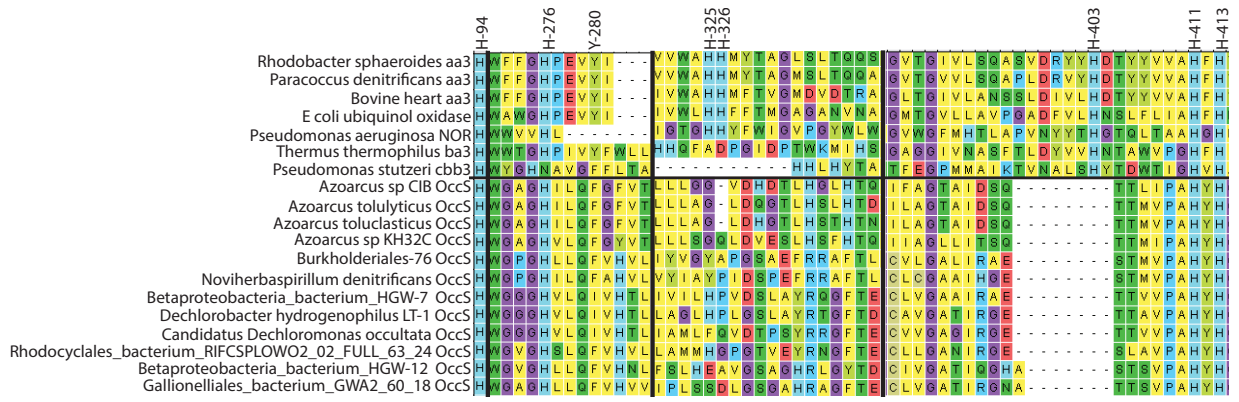

Figure S6. Shared features of the OccS conserved domain in selected *Betaproteobacteria*. Alignment of conserved cofactor-binding (heme a, a_3, and Cu_B) histidines and select D and K proton channel ligands for members of the cytochrome c oxidase subunit I family compared to OccS. Numbering is for *Paracoccus denitrificans*.

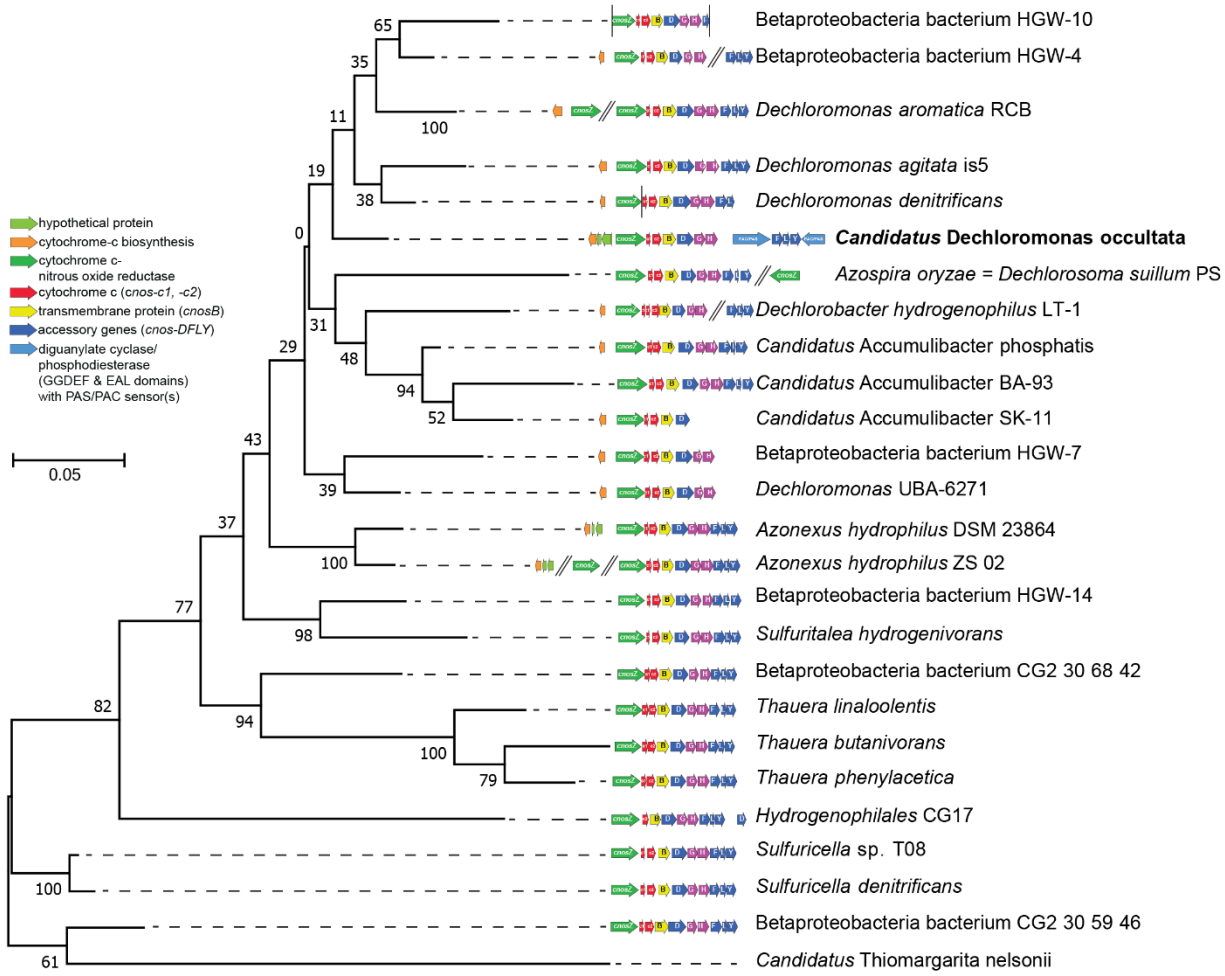

Figure S7. Phylogeny of cytochrome-nitrous oxide reductase (cNosZ) genes and synteny of the synteny of cNosZ loci. The tree represents the evolutionary history of the cNosZ protein from "*Ca*. D. occultata" in relationship to other cNosZ homologs from *Beta*- and *Gammaproteobacteria*. Accession numbers are given in Table 2. Branch lengths represent substitutions per site. Next to each branch we show the genomic organization of cNosZ and neighboring genes in each strain, color-coded by function.

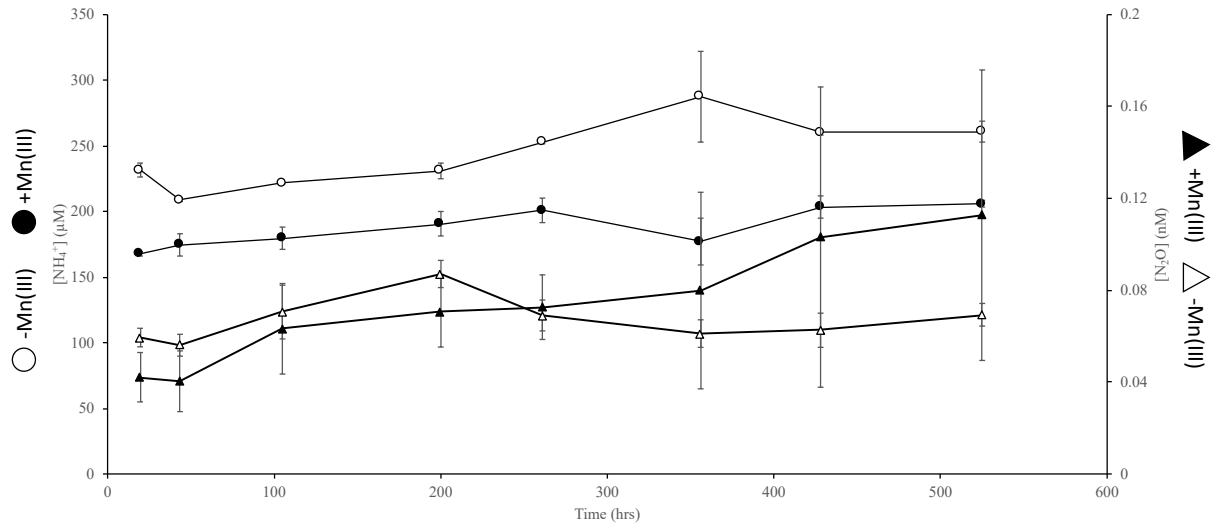

Figure S8. Abiotic reactions between Mn(III) and NH_4^+. Concentrations of NH_4^+ (circles) and N_2O (triangles) from 0.2 mM NH_4^+ added to abiotic treatments with (1 mM; closed symbols) or without (open symbols) added Mn(III) pyrophosphate. Error bars represent standard error where n=3 (N_2O) or n=2 (NH_4^+).

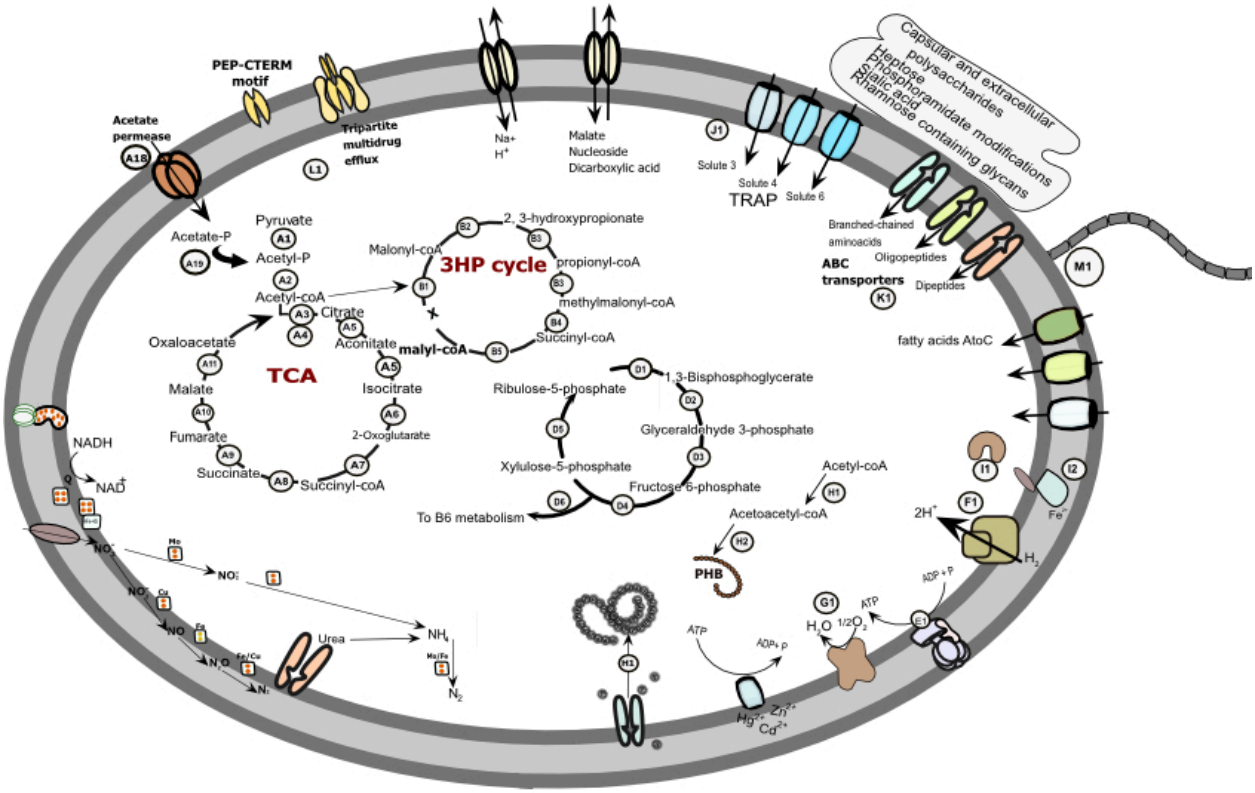

Figure S9. "*Candidatus* Dechloromonas occultata" genomic potential and gene expression during Mn(III) reduction. Key genes involved in central and secondary metabolism including carbon and nitrogen metabolism, energy generation, and environmental sensing are shown. Numbers correspond to proteins compiled in table S4.

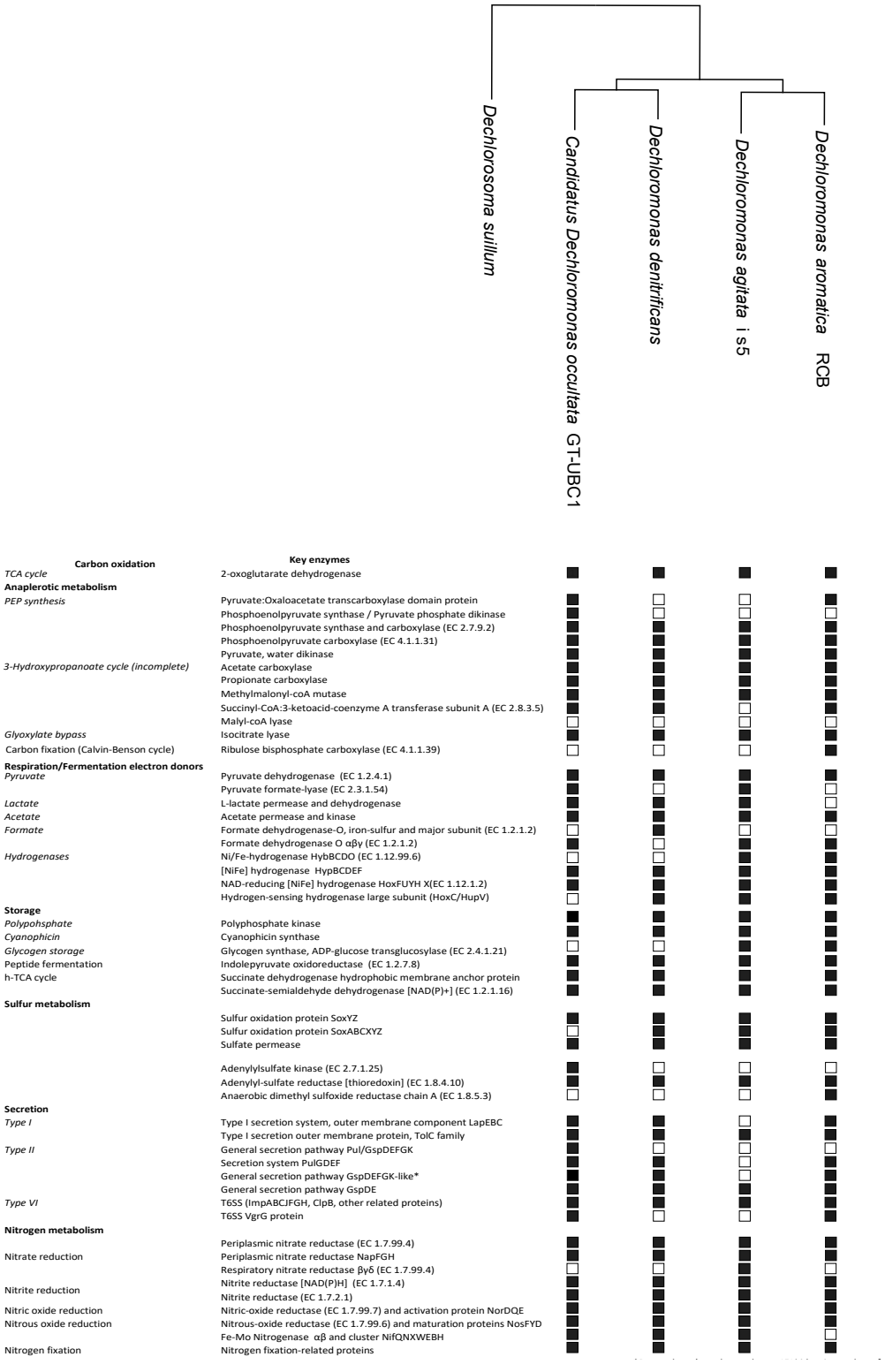

Figure S10. Comparison of carbon, nitrogen and respiratory metabolic pathways for the *Dechloromonas* genus based on three representative strains and "*Ca.* D. occultata".

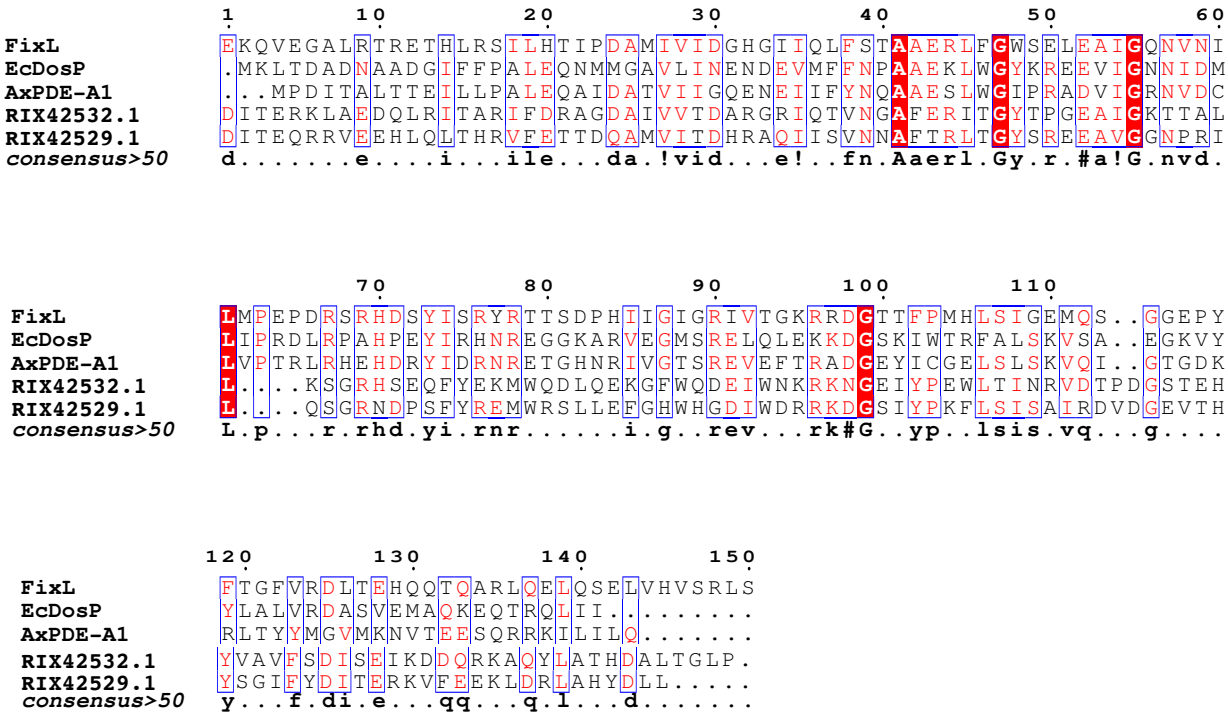

298

299 **Figure S11. Conserved features of sensor RIX42529 and betaproteobacterial homologs.**

300 Alignment of conserved heme-binding histidines for members of the PAS-O_2 sensor family

301 (FixL, EcDosP, and AxPDE-A1) and two predicted PAS sensors in "*Ca*. D. occultata"

302 (RIX42532 and RIX42529).

References

1 Aigle A, Bonin P, Iobbi-Nivol C, Mejean V, Michotey V (2017). Physiological and transcriptional approaches reveal connection between nitrogen and manganese cycles in Shewanella algae C6G3. *Sci Rep* **7:** 44725.

2 Aziz RK, Bartels D, Best AA, DeJongh M, Disz T, Edwards RA *et al* (2008). The RAST Server: rapid annotations using subsystems technology. *BMC genomics* **9:** 75.

3 Badalamenti JP, Summers ZM, Chan CH, Gralnick JA, Bond DR (2016). Isolation and genomic characterization of 'Desulfuromonas soudanensis WTL', a metal-and electrode-respiring bacterium from anoxic deep subsurface brine. *Frontiers in microbiology* **7**.

4 Bankevich A, Nurk S, Antipov D, Gurevich AA, Dvorkin M, Kulikov AS *et al* (2012). SPAdes: a new genome assembly algorithm and its applications to single-cell sequencing. *Journal of computational biology* **19:** 455-477.

5 Blomberg MR, Siegbahn PE (2014). Proton pumping in cytochrome c oxidase: Energetic requirements and the role of two proton channels. *Biochimica et Biophysica Acta (BBA)-Bioenergetics* **1837:** 1165-1177.

6 Boumaiza H, Coustel R, Despas C, Ruby C, Bergaoui L (2018). Interaction of ammonium with birnessite: Evidence of a chemical and structural transformation in alkaline aqueous medium. *J Solid State Chem* **258:** 543-550.

7 Bray MS, Wu J, Reed BC, Kretz CB, Belli KM, Simister RL *et al* (2017). Shifting microbial communities sustain multi-year iron reduction and methanogenesis in ferruginous sediment incubations. *Geobiology* **15:** 678-689.

8 Brettin T, Davis JJ, Disz T, Edwards RA, Gerdes S, Olsen GJ *et al* (2015). RASTtk: a modular and extensible implementation of the RAST algorithm for building custom annotation pipelines and annotating batches of genomes. *Scientific reports* **5:** 8365.

9 Burnes BS, Mulberry MJ, DiChristina TJ (1998). Design and application of two rapid screening techniques for isolation of Mn (IV) reduction-deficient mutants of *Shewanella putrefaciens*. *Applied and environmental microbiology* **64:** 2716-2720.

10 Choi H, Kim S, Fermin D, Tsou C-C, Nesvizhskii AI (2015). QPROT: Statistical method for testing differential expression using protein-level intensity data in label-free quantitative proteomics. *Journal of proteomics* **129:** 121-126.

11 Crowe SA, Jones C, Katsev S, Magen Cd, O'Neill AH, Sturm A *et al* (2008). Photoferrotrophs thrive in an Archean Ocean analogue. *Proceedings of the National Academy of Sciences* **105:** 15938-15943.

12 Crowe SA, Canfield DE, Mucci A, Sundby B, Maranger R (2012). Anammox, denitrification and fixed-nitrogen removal in sediments from the Lower St. Lawrence Estuary. *Biogeosciences* **9:** 4309-4321.

13 Dedysh SN, Dunfield PF, Trotsenko YA (2004). Methane utilization by Methylobacterium species: new evidence but still no proof for an old controversy. *Int J Syst Evol Microbiol* **54:** 1919-1920.

14 Emerson D, Floyd MM (2005). Enrichment and isolation of iron-oxidizing bacteria at neutral pH. *Method Enzymol* **397:** 112-123.

15 Eng JK, Jahan TA, Hoopmann MR (2013). Comet: an open-source MS/MS sequence database search tool. *Proteomics* **13:** 22-24.

16 Gardy JL, Laird MR, Chen F, Rey S, Walsh C, Ester M *et al* (2004). PSORTb v. 2.0: expanded prediction of bacterial protein subcellular localization and insights gained from comparative proteome analysis. *Bioinformatics* **21:** 617-623.

17 Gonska N, Young D, Yuki R, Okamoto T, Hisano T, Antonyuk S *et al* (2018). Characterization of the quinol-dependent nitric oxide reductase from the pathogen Neisseria meningitidis, an electrogenic enzyme. *Scientific reports* **8:** 3637.

18 Green PN, Bousfield IJ (1983). Emendation of Methylobacterium Patt, Cole, and Hanson 1976, Methylobacterium-Rhodinum (Heumann 1962) Comb-Nov-Corrig, Methylobacterium-Radiotolerans (Ito and Iizuka 1971) Comb-Nov-Corrig, and Methylobacterium-Mesophilicum (Austin and Goodfellow 1979) Comb-Nov. *Int J Syst Bacteriol* **33:** 875-877.

19 Guanghuan G, Jianqiang Z, Aixia C, Bo H, Ying C, Kun G *et al* (2018). Nitrogen Removal and Nitrous Oxide Emission in an Anaerobic/Oxic/Anoxic Sequencing Biofilm Batch Reactor. *Environmental Engineering Science* **35:** 19-26.

20 Hansen JW, Thamdrup B, Jørgensen BB (2000). Anoxic incubation of sediment in gas-tight plastic bags: a method for biogeochemical process studies. *Marine Ecology Progress Series* **208:** 273-282.

21 Jones C, Crowe SA, Sturm A, Leslie KL, MacLean LCW, Katsev S *et al* (2011). Biogeochemistry of manganese in ferruginous Lake Matano, Indonesia. *Biogeosciences* **8:** 2977-2991.

22 Jones DT, Taylor WR, Thornton JM (1992). The rapid generation of mutation data matrices from protein sequences. *Bioinformatics* **8:** 275-282.

23 Kalyuzhnaya MG, Hristova KR, Lidstrom ME, Chistoserdova L (2008). Characterization of a novel methanol dehydrogenase in representatives of Burkholderiales: Implications for environmental detection of methylotrophy and evidence for convergent evolution. *J Bacteriol* **190:** 3817-3823.

24 Kleiner M, Wentrup C, Lott C, Teeling H, Wetzel S, Young J *et al* (2012). Metaproteomics of a gutless marine worm and its symbiotic microbial community reveal unusual pathways for carbon and energy use. *Proceedings of the National Academy of Sciences* **109:** E1173-E1182.

25 Kostka JE, Luther III GW, Nealson KH (1995). Chemical and biological reduction of Mn (III)-pyrophosphate complexes: potential importance of dissolved Mn (III) as an environmental oxidant. *Geochimica et Cosmochimica Acta* **59:** 885-894.

26 Kumar S, Stecher G, Tamura K (2016). MEGA7: Molecular Evolutionary Genetics Analysis version 7.0 for bigger datasets. *Molecular biology and evolution* **33:** 1870-1874.

27 Kuntz L, Laakso T, Schrag D, Crowe S (2015). Modeling the carbon cycle in Lake Matano. *Geobiology* **13:** 454-461.

28 Lee MD (2019). GToTree: a user-friendly workflow for phylogenomics. *Bioinformatics*.

29 Liu Y, Peng L, Guo J, Chen X, Yuan Z, Ni B-J (2015). Evaluating the Role of Microbial Internal Storage Turnover on Nitrous Oxide Accumulation During Denitrification. *Scientific Reports* **5:** 15138.

30 MacLean B, Tomazela DM, Abbatiello SE, Zhang S, Whiteaker JR, Paulovich AG *et al* (2010). Effect of collision energy optimization on the measurement of peptides by selected reaction monitoring (SRM) mass spectrometry. *Analytical chemistry* **82:** 10116-10124.

31 Nesvizhskii AI, Keller A, Kolker E, Aebersold R (2003). A statistical model for identifying proteins by tandem mass spectrometry. *Analytical chemistry* **75:** 4646-4658.

32 Nunn BL, Slattery KV, Cameron KA, Timmins-Schiffman E, Junge K (2015). Proteomics of *Colwellia psychrerythraea* at subzero temperatures–a life with limited movement, flexible membranes and vital DNA repair. *Method Enzymol* **17:** 2319-2335.

33 Overbeek R, Olson R, Pusch GD, Olsen GJ, Davis JJ, Disz T *et al* (2013). The SEED and the Rapid Annotation of microbial genomes using Subsystems Technology (RAST). *Nucleic acids research* **42:** D206-D214.

34 Parks DH, Imelfort M, Skennerton CT, Hugenholtz P, Tyson GW (2015). CheckM: assessing the quality of microbial genomes recovered from isolates, single cells, and metagenomes. *Genome Res* **25:** 1043-1055.

35 Rambaut A (2012). FigTree: Tree Figure Drawing Tool. Available at http://tree.bio.ed.ac.uk/software/figtree/.

36 Schloss PD, Westcott SL, Ryabin T, Hall JR, Hartmann M, Hollister EB *et al* (2009). Introducing mothur: open-source, platform-independent, community-supported software for describing and comparing microbial communities. *Appl Environ Microbiol* **75:** 7537-7541.

37 Seemann T (2014). Prokka: rapid prokaryotic genome annotation. *Bioinformatics* **30:** 2068-2069.

38 Shimizu T, Huang D, Yan F, Stranava M, Bartosova M, Fojtíková V *et al* (2015). Gaseous O2, NO, and CO in signal transduction: structure and function relationships of heme-based gas sensors and heme-redox sensors. *Chemical reviews* **115:** 6491-6533.

39 Van Aken B, Peres CM, Doty SL, Yoon JM, Schnoor JL (2004). Methylobacterium populi sp. nov., a novel aerobic, pink-pigmented, facultatively methylotrophic, methane-utilizing bacterium isolated from poplar trees (Populus deltoides×nigra DN34). *International Journal of Systematic and Evolutionary Microbiology* **54:** 1191-1196.

40 Veltri D, Wight MM, Crouch JA (2016). SimpleSynteny: a web-based tool for visualization of microsynteny across multiple species. *Nucleic acids research* **44:** W41-W45.

41 Wattam AR, Abraham D, Dalay O, Disz TL, Driscoll T, Gabbard JL *et al* (2013). PATRIC, the bacterial bioinformatics database and analysis resource. *Nucleic acids research* **42:** D581-D591.

42 Wu Y-W, Simmons BA, Singer SW (2015). MaxBin 2.0: an automated binning algorithm to recover genomes from multiple metagenomic datasets. *Bioinformatics* **32:** 605-607.

43 Zorz JK, Kozlowski JA, Stein LY, Strous M, Kleiner M (2018). Comparative Proteomics of Three Species of Ammonia-Oxidizing Bacteria. *Frontiers in Microbiology* **9:** 938.